ACTINIDE RESEARCH QUARTERLY

Ac Th Pa U Np Pu Am Cm Bk Cf Es Fm Md No Lr

Third Quarter 2020

Plutonium Nuclear Magnetic Resonance

Los Alamos NATIONAL LABORATORY

Foreword

In this issue we are proud to feature articles from a variety of Seaborg-funded Fellows at Los Alamos National Laboratory (LANL), including research from four recent Seaborg postdocs.

In a historical experiment in 2012, LANL researchers detected a spectroscopic signal for plutonium-239 that had never been determined before. Specifically, they used nuclear magnetic resonance to probe a sample of plutonium dioxide, demonstrating for the first time that this powerful analytical technique could be used for actinide materials relevant to nuclear power and the nation's nuclear stockpile. The lead scientist in this project, Hiroshi Yasuoka, returned to LANL last summer as a visiting scientist and Seaborg Scholar to continue his work in this area. His article on *p2* gives an overview to this exciting work, showing the past successes and future challenges of this technology.

The properties of actinide oxides as nuclear fuel materials are studied in two articles in this issue. The first, by Nestor Aguirre, uses theoretical methods to examine the properties of these materials in nanoparticulate form (*p8*). The second, by Jordan Evans, explores the fundamental properties of uranium-dioxide and -silicide from the perspective of developing accident-tolerant nuclear fuels (*p21*).

One of the great challenges in the nuclear energy industry is waste disposal, which often contains an inseparable mixture of non-radioactive lanthanide and radioactive actinide isotopes. In an article on *p12*, David Baumann describes the chemical synthesis of a new class of potential actinide chelators for use in actinide separations.

Taylor Jacobs, now a scientist at LANL, is primarily interested in microstructure-property relationships in plutonium. As he explains: “Understanding the nature of radiation damage in plutonium is of great importance as we seek to safely maintain our aging nuclear weapons stockpile without nuclear testing.” His article on *p16* details how internal friction can be used as an effective characterization technique to probe crystalline defects and structures in plutonium that are difficult to account for with more traditional methods.

Reading about scientific results in a publication such as ARQ doesn't always tell us the whole picture. It takes a village to perform cutting-edge research, especially with restricted materials such as the atinide elements. In light of this, we end the issue with an employee spotlight by Maureen Lunn (ALD-WP) on Sheldon Apgar of the Actinide Materials Processing & Power (AMPP-4) group at TA-55 (*p27*) where he works as a designer/drafter and has a knack for solving glovebox problems.

Owen Summerscales
Editor

About the cover: When placed in a magnetic field, charged particles will precess about the field. In nuclear magnetic resonance (NMR), the charged nucleus of an atom will exhibit precessional motion at a characteristic frequency, which can ultimately yield information about the material at an atomic scale. This precession is often represented by the classical spinning top analogy (nuclear "spins" are a quantum phenomenon however, therefore this analogy, while useful, has limitations). In the case of plutonium-239, its spin-½ nucleus should make it a good candidate for NMR in principle, yet it has resisted spectroscopic detection for decades. Read the article by Yasuoka on *p2* for the full story.

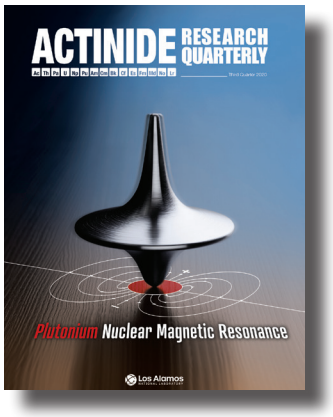

Contents

Employee Spotlight **27**

MEASUREMENT METHODS

2 Probing Plutonium Materials with Magnetic Resonance
Hiroshi Yasuoka

ACTINIDE THEORY

8 Theoretical Description of Actinide Dioxide Nanoparticles
Nestor Aguirre

CHEMISTRY

12 Creating a New Class of Actinide Chelators
David O. Baumann

MATERIALS SCIENCE & METALLURGY

16 Developing Internal Friction Capabilities for Plutonium
Taylor R. Jacobs

NUCLEAR ENGINEERING & FUELS

21 Developing Accident-Tolerant Nuclear Fuels: Temperature-Dependent Properties of UO_2 and U_3Si_2
Jordan A. Evans

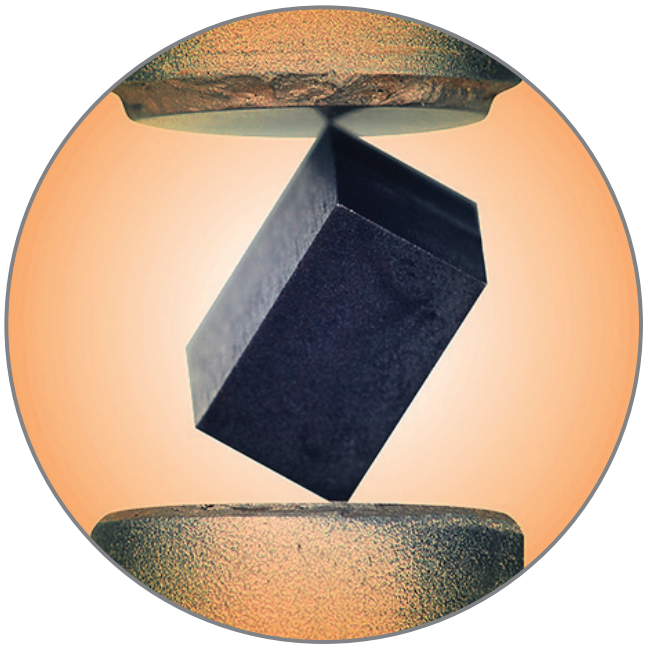

Probing Plutonium Materials with Magnetic Resonance

Hiroshi Yasuoka

MPA-CMMS, Los Alamos National Laboratory, Los Alamos, New Mexico, USA, and Max-Planck-Institute for Chemical Physics of Solids MPI-CPfS, Dresden, Germany

Visiting scientist Hiroshi Yasuoka was a Seaborg Scholar from April–August 2019 and previously from November 2010–September 2011. Over his long career he has notably held the position of Professor at the Institute for Solid State Physics at the University of Tokyo in Japan, and worked at the Japan Atomic Energy Agency, among numerous other positions. Some of his awards include the 24th Nishina Memorial Award (1997) and the Honorary Award of the Millennium Science Forum, presented by HRH the Princess Royal at British Embassy, Tokyo, 1999. His research interests cover areas such as superconductivity, actinide materials, and nuclear magnetic resonance.

We use nuclear magnetic resonance (NMR) spectroscopy on solid materials to understand their chemical and physical properties. Of most interest are those containing isotopes with a nuclear spin of ½, such as hydrogen and carbon, due to the detailed information that can be obtained by studying this type of nucleus. The spin-½ nucleus of ^{239}Pu meanwhile has resisted attempts by researchers to observe its direct signature because of the unusually large internal magnetic field at the nuclear site that arises from the strong interaction between nuclear spins and the orbital current of electrons. This effect causes an extraordinarily fast nuclear relaxation time, making it very difficult to directly observe ^{239}Pu signals except under certain circumstances. This work has been further constrained because plutonium is a federally controlled substance and facilities which can handle such "hot" materials are limited.

In 2012, a historical observation of the ^{239}Pu NMR signal in PuO_2 at Los Alamos National Laboratory (LANL) was made, followed by the second observation of this nucleus in putative topological insulators PuB_4/PuB_6 by the same group in 2018. Having determined the ^{239}Pu isotope's signature (namely, the nuclear gyromagnetic ratio $^{239}\gamma_n$) we are now in a favorable position to study the structure and chemical bonding of plutonium compounds by using this NMR technique as a local probe. It can also be used to study both the chemical properties and self-radiation effects in nuclear fuels, nuclear waste, and organometallic molecules, and the physical properties of magnets, superconductors, and other plutonium-based correlated electron materials. This short article provides an overview of ^{239}Pu-NMR spectroscopic research at LANL and an outlook for its future applications.

Basic aspects of NMR

A nucleus with a non-zero spin possesses a magnetic moment, like a magnetic compass. Quantum mechanics tells us that in the presence of a magnetic field the nuclear magnetic energy levels split to equally-spaced energy levels by the Zeeman interaction. In an NMR experiment we apply an oscillatory field with a frequency corresponding to the energy difference. The resonance condition is expressed by a linear relation between frequencies and fields with a proportional constant γ_n, the nuclear gyromagnetic ratio, which is the "fingerprint" of a specific nucleus.

In materials, nuclear spins sense an additional "internal" magnetic field arising primarily from an interaction with their electronic environment (hyperfine interaction) and with each other. The static component of the internal field results in a change of the measured resonance frequency—the relative shift of the resonance frequency is called the Knight shift. The fluctuating component of the internal field meanwhile is responsible for the relaxation of nuclear spins. In particular, the nuclear spin-lattice relaxation time T_1 (or the relaxation rate, $1/T_1$) is an important parameter related to the dynamical response of magnetic susceptibility, and its temperature dependence gives us a quantitative measure of the low-energy magnetic excitations.

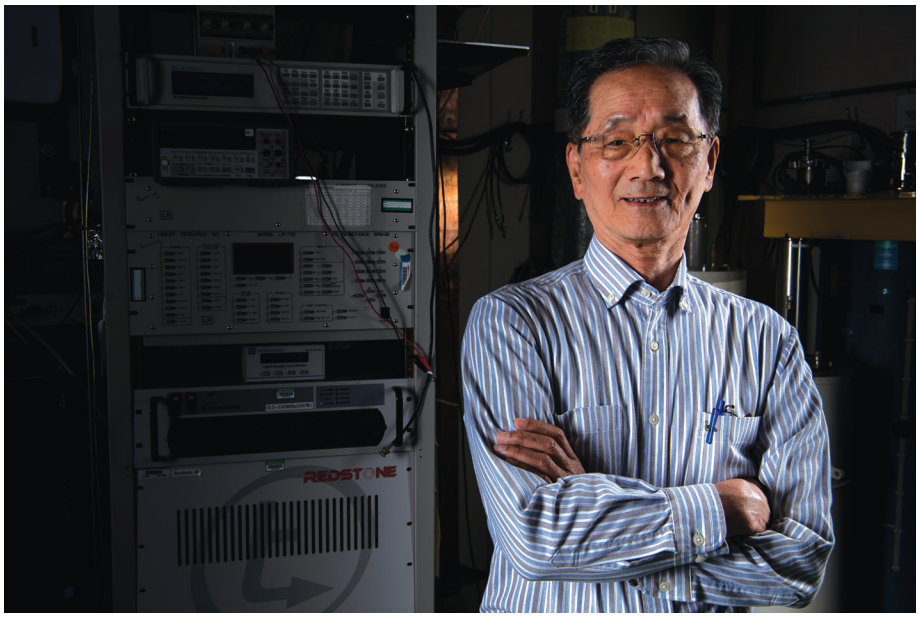

The first observation of a ^{239}Pu NMR signal

The search for plutonium NMR signals in liquid or solid phases has focused primarily on spin-½ ^{239}Pu; nevertheless, this was not observed until 2012. The signal remained elusive for two reasons: first, an extremely strong hyperfine interaction between electron and nuclear spins, due to unpaired 5f electrons, gives rise to a large internal magnetic field (~100 T) at the nuclear site. This internal field shifts the resonance frequency by several orders of magnitude, and the nuclear spin-relaxation time becomes exceedingly fast (less than one microsecond), making any measurements very challenging. Second, there was a range of values in the literature reported for the ^{239}Pu nuclear moment giving a large uncertainty to the nuclear gyromagnetic ratio.

To overcome the limitations imposed by the strong hyperfine interaction, a search for the ^{239}Pu NMR signal in PuO_2 was most plausible because the Pu^{4+} ion in PuO_2 is in a tetravalent state and has cubic local symmetry. Although PuO_2 is known to have a variable stoichiometry of oxygen, a fully oxidized and well characterized sample should contain Pu^{4+} ($5f^4$, $^5I_4$) ions with a non-magnetic, singlet ground state in a cubic crystalline electric field. With the first excited magnetic state being higher in energy than the ground state, the Pu^{4+} ions should be non-magnetic below room temperature, which is reflected by the observed temperature-independent magnetic susceptibility. To address the lack of accurate data for the nuclear gyromagnetic ratio, the external magnetic field was swept at a constant frequency across a wide range of expected γn values. This approach was successful—by mapping the external field dependence of the measured resonance frequency, we determined the nuclear gyromagnetic ratio $^{239}\gamma_n(PuO_2)$ to be $2\pi \times 2.856$ MHz/T (Fig. l). Assuming a free-ion value for the Pu^{4+} hyperfine coupling constant, we determined the isolated "bare" value of the gyromagnetic ratio to be $2\pi \times 2.29$ MHz/T, corresponding to a ^{239}Pu nuclear magnetic moment of 0.15 μ_N (where μ_N is the nuclear magneton).

Of course, this discovery has not suddenly transformed Pu NMR spectroscopy into a trivial affair. Challenges remain, and as of now the pool of candidate compounds for future development is rather limited because most of the known Pu compounds are strongly magnetic and their short nuclear relaxation times prevent

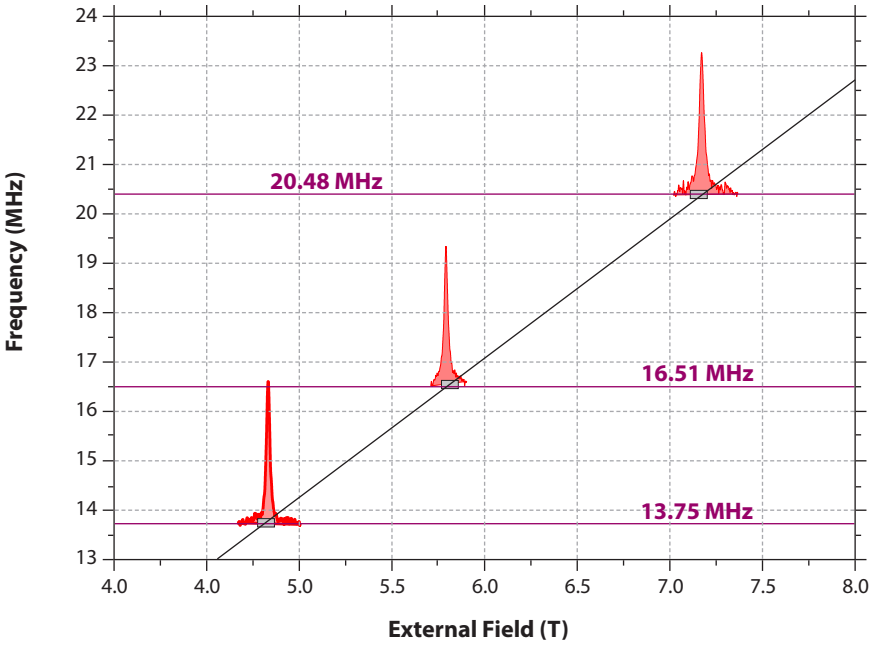

Figure 1. This data plot shows how the ^{239}Pu nuclear gyromagnetic ratio γ_n was determined. This was the first time this important parameter had been obtained for this isotope and will guide future research in the area. The frequency-field diagram of field-swept ^{239}Pu NMR spectra obtained at 3.95 K in $PuO_{2.01}$ for constant frequencies of 13.75, 16.51, and 20.48 MHz. The peak frequencies are promotional to the external filed, and from the slope we determined $^{239}\gamma_n = 2.856 \pm 0.001$ MHz/T.

us from observing any signals. Nevertheless, the impact of this discovery is both profound and multi-faceted. Ending a decade-long search, it has provided a proof-of-concept, rendering Pu NMR spectroscopy a reality rather than an impossibility. We now have insight into the gyromagnetic ratio values and nuclear magnetic moment of ^{239}Pu, which provides a clear path forward. Especially in view of the complexity of these compounds and their technological importance, directly observing the consequences of plutonium's 5f electrons at the atomic and structural unit-cell scales using NMR spectroscopy could potentially prove a particularly powerful tool for solid-state physics, chemistry, and materials science.

^{239}Pu NMR signal in PuB_4

In 2018 we reported the second-ever observation of a ^{239}Pu NMR signal. We detected this in bulk and single-crystal plutonium tetraboride (PuB_4), which has been investigated as a potential correlated topological insulator. The NMR results have provided unique f-electron physics and insight into the bulk gap-like behavior of the transport properties in this material. The temperature dependence of the ^{239}Pu Knight shift combined with a relatively long nuclear spin-lattice relaxation time indicates that PuB_4 adopts a non-magnetic state with gap-like behavior consistent with the theoretical band structure calculations. These results imply that PuB_4 is a good candidate as a topological insulator. Simultaneously we observed an excess nuclear relaxation process below a characteristic temperature, typically ~100 K (Fig. 2), in which the high-temperature activated process crossed over into a low-temperature process of unknown character. This is a common feature with other topological insulators and Weyl semi-metals (e.g., SmB_6, YbB_{12}, and TaP); the mechanism is still an open question. Another exciting finding is that the Knight shift, which predominantly arises from the orbital hyperfine interaction, strongly depends on the chemical coordination and the nature of electronic states (Fig. 3). We found that ^{239}Pu NMR spectroscopy is quite sensitive to f-electron configuration (metallic or ionic), nature of the chemical bond, and the environment around the Pu ions. This gives a new path for the exploration of self-radiation damage and accompanying aging effects using ^{239}Pu NMR spectroscopy as a local probe.

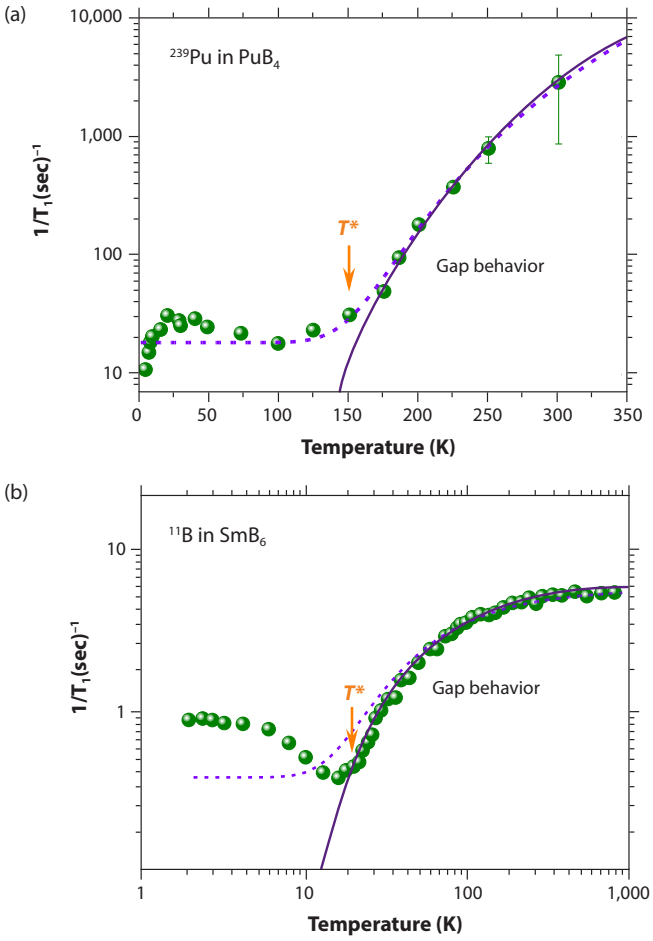

Figure 2. Temperature dependence of (a) the nuclear magnetic relaxation rate for ^{239}Pu in PuB_4 and (b) for ^{11}B in SmB_6, a typical topological insulator. For both cases the data shows an activation type increase above T* (the crossover temperature between two processes) due to excitations through the gap characteristic to insulators with a band gap (solid line). Below T* the data deviate from high-temperature activation type process and an excess relaxation process sets in (dashed line).

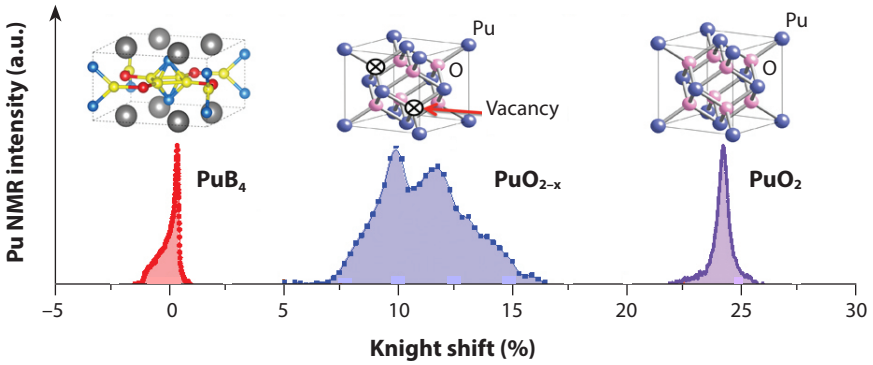

Figure 3. ^{239}Pu NMR data for PuO_2 and PuO_{2-x} (insulators) and PuB_4 (metallic with band gap). The spectral intensity is plotted against Knight shift which is the sum of the negative contribution of the spin component and a positive orbital component of the 5f electrons. The Knight shift is defined as the fractional change of the resonance field due to the hyperfine field at the nuclear site. This shows that ^{239}Pu NMR is sensitive to different materials, indicating that it depends strongly on the f-electron configuration, nature of chemical bond, and environment around the Pu atoms. The PuO_{2-x} spectrum shows a satellite structure reflecting the variations in local environment around the oxygen vacancies.

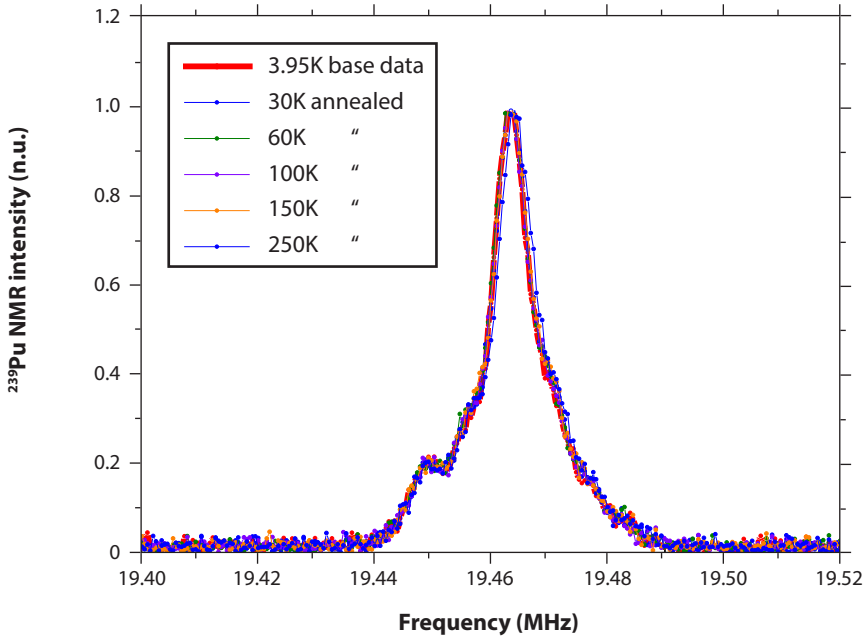

Figure 4. ^{239}Pu NMR spectra for a PuB_4 single crystal with an external field applied parallel to the b-axis (base data at 3.95K). The spectrum consisted of a major resonance, ascribed to Pu atoms without any structural damage in the local environment, surrounded by several satellites. These secondary peaks are due to variations in the surrounding atomic structure or defects due to the radiation damage (environment effects). Isochronal annealing effects on the ^{239}Pu NMR spectra measured at the base temperature of 3.95 K are also shown. Annealing was performed at 20, 60, 100, 150 and 250 K for 12 hours. There was no appreciable effect observed, suggesting that the activation energy of annealing is much higher than room temperature.

Self-damage and isochronal annealing effects on local structure

Understanding the mechanisms of self-damage and aging effects in radioactive materials is a matter of significant concern in the actinide science community. In principle, ^{239}Pu NMR spectroscopy could be a very effective technique to solve these problems because NMR spectra can be very sensitive to local environment changes, such as those caused by radiation self-damage. We can expect a split or broadened structure in the spectra, depending on the degree of local radiation damage. We observed such an effect on the ^{239}Pu NMR spectrum of a PuB_4 single crystal which was stored at 3.95 K for nearly one month in order to accumulate damage (Fig. 4). We subsequently observed a satellite structure dependent on the local environment which might arise from Pu sites surrounding structurally damaged areas. Although we do not know which satellite peaks correspond to which areas, this spectrum encouraged us to perform another experiment in order to see if annealing would "heal" the damaged sites. The isochronal annealing results we have obtained so far are shown in the same figure. After annealing at elevated temperatures, the spectrum does not change and there are essentially no effects on the annealing temperature up to 250 K. This is because the melting point of PuB_4 is so high (ca. 20,430°C) therefore the annealing temperature is expected to be much higher than room temperature. Nevertheless, further investigations are warranted for δ-Pu metal or PuO_2 on which macroscopic measurements have shown the annealing effect at much lower temperatures (typically less than room temperature).

Summary and outlook

In view of the complexity of Pu compounds and their technological importance, directly observing the consequences of plutonium's 5f electrons at the atomic and structural unit-cell scales using the ^{239}Pu NMR spectroscopy could potentially prove a particularly powerful tool for the study of plutonium solid-state physics, chemistry, and materials science. Seven years passed between the first observation of the ^{239}Pu NMR signal, in PuO_2, and the second, in PuB_4. During this time we have attempted to observe signals in several plausible materials, such as $PuCoGa_5$, $PuPt_3$, and $[(Me)_4N]_2PuCl_6$, but no signatures were observed. Nevertheless, our understanding of ^{239}Pu NMR characteristics has greatly advanced. There are many areas from both physics and chemistry perspectives that future work could build on these advances:

1. The Knight shift strongly depends on the nature of the chemical bonding between Pu and ligand atoms (ranging from 0 to +25 %). Therefore the observation of ^{239}Pu NMR signals in other compounds of interest is important not only to understand basic electronic states but also to elucidate the details of chemical bonding (compounds of interest include: Pu metal (Ga-stabilized δ-Pu), PuB_6 (topological insulator), $PuCoGa_5$ (superconductor), PuF_4, etc.).
2. Now we know NMR parameters for both ^{235}U and ^{239}Pu, a very interesting project is the study of the UO_2/PuO_2 mixed oxide system (MOX) to characterize the phase stability and thermoelectric properties.
3. From a pure physics perspective, the excess relaxation process observed below T* in PuB_4 should be clarified because this is a rather common feature observed in various topological insulators or semi-metals (e.g., SmB_6, YbB_{12}, TaP, etc.). From the external field and pressure dependence of $1/T_1$, we could understand this phenomenon in more detail.
4. Future work studying self-radiation damage and aging effects should be continued using δ-Pu or PuO_2 rather than PuB_4. Because of its high melting point, annealing temperatures are much higher than room temperature and therefore we have concluded that PuB_4 is a poor choice of material for this type of study. A better choice of materials could allow us to observe how the ^{239}Pu NMR spectra change as a function of annealing and consequently obtain the thermodynamic data of the damaged lattice by radiation and annealing effects.

Finally, I should emphasize that although we now have an excellent microscopic tool to study plutonium compounds which have the most fascinating and unique physical and chemical properties, we also need to have strong collaborations in the form of teamwork between synthetic scientists and theoretical physicists and chemists to support this effort.

Further reading:

1. *G. Koutroulakis, H. Yasuoka, "Actinides: Nuclear magnetic resonance," Encyclopedia of Inorganic and Bioinorganic Chemistry, 2018, John Wiley & Sons, Ltd.*
2. *H. Yasuoka, G. Koutroulakis, H. Chudo, S. Richmond, D.K. Veirs, A.I. Smith, E.D. Bauer, J.D. Thompson, G.D. Jarvinen, D.L. Clark, "Observation of ^{239}Pu nuclear magnetic resonance," Science, 2012, 336, 901.*
3. *A. P. Dioguardi, H. Yasuoka, S. M. Thomas, H. Sakai, S. K. Cary, S. A. Kozimor, T. E. Albrecht-Schmitt, H. C. Choi, J.-X. Zhu, J. D. Thompson, E. D. Bauer, F. Ronning, "^{239}Pu nuclear magnetic resonance in the candidate topological insulator PuB_4," Phys. Rev., 2019, B99, 035104.*
4. *M. Takigawa, H. Yasuoka, Y. Kitaoka, T. Tanaka, H. Nozaki, Y. Ishizawa, "NMR study of a valence fluctuating compound SmB_6," J. Phys. Soc. Jpn., 1981, 50, 2525.*
5. *H. Yasuoka, T. Kubo, Y. Kishimoto, D. Kasinathan, M. Schmidt, B. Yan, Y. Zhang, H. Tou, C. Felser, A.P. Mackenzie, M. Baenitz, "Emergent Weyl fermion excitations in TaP explored by ^{181}Ta quadrupole resonance," Phys. Rev. Lett., 2017, 118, 236403.*

Acknowledgments

This project was supported by the LANL Laboratory Directed Research and Development program and the Glenn T. Seaborg Institute. I thank the following for all their contributions: A. Mounce, A.P. Dioguardi, S.B. Blackwell, S. Thomas, S.M. Thomas, S.K. Cary, S.A. Kozimor, A.T.E. Albrecht-Schmitt, J.D. Thompson, E.D. Bauer, H.C. Choi, J.-X. Zhu, F. Ronning, D.L. Clark.

Nestor Aguirre was a Seaborg Fellow from December 2017–October 2019. He holds a BSc and MSc in theoretical chemistry from the National University of Colombia, and a PhD from the National Research Council in Spain. He worked as a postdoctoral research associate at the Autonomous University of Madrid, before moving to LANL as a postdoctoral fellow. He has developed and applied computational chemistry methods in many different fields, such as: molecular fragmentation processes induced by collisions, high-order harmonic generation, and global optimizations, particularly applied to energy minimum configuration and parameter optimization of electronic structure methods for actinide systems. He is now a Scientific Software Developer at Software for Chemistry & Materials (SCM) based in the Netherlands.

Theoretical Description of Actinide Dioxide Nanoparticles

Nestor Aguirre
Los Alamos National Laboratory, Los Alamos, New Mexico 87545

Metal oxides play an important role in chemistry, physics, and materials science. They can adopt a variety of structural geometries with electronic structures that can show a range of behaviors through metallic, semiconducting, or insulating, forming a large diversity of oxide compounds. In technological applications, metal oxides are used in fields ranging from sensors, fuel cells, catalysts, and the fabrication of microelectronic circuits, among others. In the field of nanotechnology, the ultimate goal is to produce nanostructures with specially tailored properties that contrast with those in the bulk. Typically, nanoparticles are defined as an agglomeration of atoms and molecules 1–100 nm in diameter. They can be comprised of one or more species of atoms (or molecules) and can exhibit a wide range of size-dependent properties. As the size of the nanoparticle is reduced to tens of nanometers or less, quantum effects can begin to play a role, which can significantly affect the material's properties, namely: structural characteristics, electronic properties, and chemical reactivity (as a consequence of the previous two effects). This makes these systems very interesting for applications in catalysis sensing, and other broad uses in materials, biology, and environment.

One of the most important properties related to nanoparticle size is stability against ionizing radiation. Experiments performed previously with nickel and platinum nanostructures have shown enhanced resistance against radiation-damage due to their nanostructures. Defects are created as radiation interacts with a material, but reducing the size of the particles below ~30 nm eliminated the creation of these defects. This is a very desirable property for actinide oxides, which have been widely used in traditional nuclear fuel fabrication and play an important role in many stages of the nuclear fuel cycle. The latter in combination with new experimental breakthroughs, such as those that have demonstrated controlled synthesis of Th(IV)-based nanoparticles, open the way to designing new nuclear fuel materials with extended lifetimes and improved performance.

Unfortunately, experimental characterization of these structures is difficult. Atomistic models are a complementary and fundamental tool to understand the properties of these systems. This type of modeling is however still a challenge from a theoretical point of view because the number of stable structures increases exponentially with the number of atoms, and typically we are interested in the lowest-energy structures. Indeed, due to the complexity of the potential energy surface of such systems it is an incredibly complicated challenge to localize the global minimum energy structure—we are looking for a proverbial needle in a haystack.

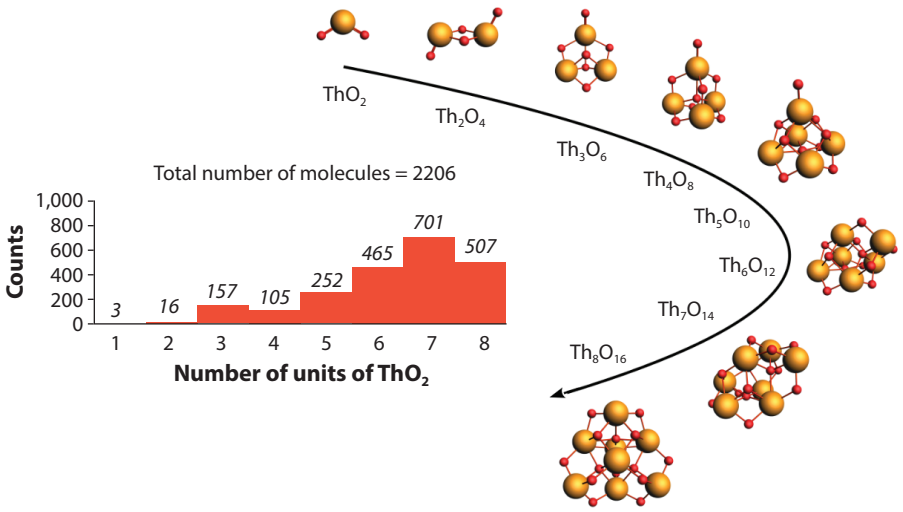

Figure 1. Lowest energy configurations for Th_nO_{2n} (n = 1–8) clusters and histogram with the total number of stable configurations explored for each size at DFT level of theory.

Theoretical modeling

Today, theoretical modeling has advanced in concert with experimental techniques in the science of nanomaterials. The development of supercomputer parallel codes has led to an increase in computational power by a factor of a million along with new algorithms for more accurate and faster calculations of quantum chemistry in the last two decades. These advancements have made it possible to perform electronic structure calculations on nanoscale systems to predict and design new functional nanomaterials.

Our main objective is to identify structural features that stabilize different cluster sizes through comparison of the global minimum structure with other local minimum structures. We expect that this analysis will shed light on the structure-stability relationship, as well as provide insight into the early stages of nucleation and the growth mechanism. In this work, we focus on stoichiometric clusters of thorium dioxide, Th_nO_{2n}. For these clusters, thorium can exist in different oxidation states ranging from II, III, and IV depending on their local structures, which by itself represents a big challenge from a computational perspective due to its intricate electronic structure. Hence, a quantum-level theory that can explicitly include electron re-arrangement is crucial.

In this work, we performed the first systematic study at the density functional theory (DFT) level of stoichiometric thorium dioxide clusters Th_nO_{2n}, where n = 1–8. The DFT results have been further validated by wave-function methods such as coupled cluster and complete active space self-consistent field (CASSCF) calculations. To explore the energy landscape of these clusters, we used a stochastic Markov chain strategy which allows for a more uniform exploration of the configuration space, and thus for the identification of stable structures with different chemical stability fingerprints. This chemically-driven geometry search algorithm in combination with the first-principle methods allows us to homogeneously screen the complex potential energy surface (PES) of actinide oxide clusters for the first time.

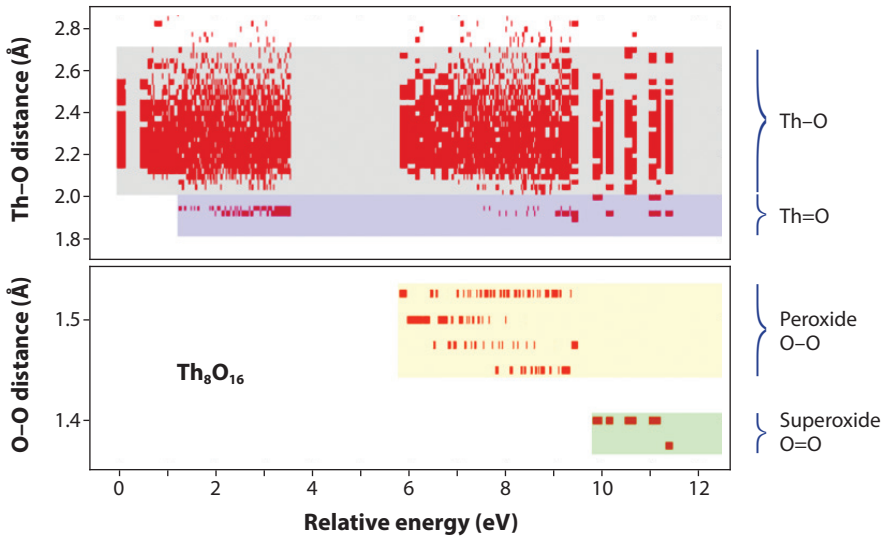

Figure 2. Scatter plot of Th–O (top), and O–O (bottom) bond distances as a function of the energy of the Th_8O_{16} clusters. Each color band represents the different energy domains of the different types of bonds that influence the stability of the Th_8O_{16} clusters. This shows how the relative energy (i.e., relative stability) is correlated with the bond distances presented in the structure for all clusters composed of eight units as a prototypical case. Each color band represents the different energy domains associated with the different types of bonds that influence the stability of the Th_8O_{16} clusters.

Thorium dioxide structure and stability

We identified more than 2,200 stable structures of Th_nO_{2n} nanoclusters (n = 1–8) within an energy range of 10 eV from the lowest configurations (Fig. 1). It was found that the presence of peroxo and superoxo groups increases the total energy of the system by at least 3.5 eV and 7 eV, respectively. Interestingly, terminally-bound oxygen groups (Th=O) arise only in cases with less than five units and only increases the energy by about 0.5 eV. In larger clusters, systems prefer configurations with bridging oxygen atom motifs (Th–O–Th). We attribute this behavior to the thorium deficiency induced by satisfying the stoichiometry.

Traditionally in chemistry it is assumed that stability largely depends on the bonds present in a molecule. Therefore we further analyzed data patterns such as geometrical motifs in order to understand the implication of the structure-stability in the crystal growth (see Fig. 2 for the relationship between relative energy/stability of a Th_8O_{16} cluster and its bond distances). A clear correlation is observed between the presence of O–O bonds and the total energy. Structures containing at least one O–O bond (peroxide) around 1.48 Å in length are destabilized by at least 6 eV, while structures containing one O=O bond (superoxide) around 1.38 Å are destabilized by at least 10 eV. Additionally, it appears that the stability of thorium dioxide nanoclusters is mostly driven by the presence—or rather the absence—of terminal oxygen atoms (Th=O) as soon as they get large enough (n > 5). Indeed, one can see that all structures containing one or more terminal oxygen groups are destabilized by at least 1 eV. For fewer than six units, the system must utilize terminal oxygen groups to compensate for its thorium deficiency.

Summary

This work is the first systematic study of structure-energy correlations in stoichiometric thorium dioxide clusters using a new generation of geometry search algorithms in combination with DFT. The relative energy of thorium dioxide clusters (ranging in size from ThO_2 and Th_8O_{16}) is found to be increased by the presence of both short O–O bonds and terminal oxygen atoms. More precisely, it is found that O–O bond distances characteristic of the peroxido (–O–O–) and superoxido (–O=O–) species tend to increase the total energy of the system by approximately 3.5 and 7 eV, respectively, while the presence of terminal oxygen atoms (=O) causes an increase of less than 1 eV. Some of these high-energy isomers can be isolated experimentally by utilizing appropriate ligands or solvent molecules. These structure-energy correlations can be exploited to design clusters with desired geometric and electronic structure features. Determining the reasons for these correlations is beyond the scope of this work but could be the topic of a future work.

Decreasing particle size from the bulk material can produce changes in thermodynamic stability. For example, phases that have a low stability in bulk materials become very stable in nanostructures, which gives us an opportunity to explore novel properties. The two main reasons for the change in behavior are an increased relative surface area and the dominance of quantum effects, due to a balance between structural transformations and surface free energy. This phenomenon has been observed previously in metal oxides such as TiO_2, VO_x, Al_2O_3, and MoO_x. We expect that for thorium oxides, the first phase transition should happen with Th_nO_{2n} clusters for n ~ 20. To model these sizes of actinide oxide clusters computationally it is necessary to develop much faster electronic structure methods such as semi-empirical parametrized density functional tight-binding, or modern data science approaches such as neural network potential-based strategies. These potentials can be used to speed up calculations for larger sized nanoscopic particles in addition to long timescale simulations. Once we reach that region, novel electronic structures and properties will arise.

From a methodological perspective, the present work shows how powerful stochastic strategies can be for determining stable isomers, including the global minimum energy structure, which is important for guiding future experimental work. In combination with molecular dynamics approaches, this method will pave the way for a better understanding of nucleation and crystal growth of actinide materials, as well as transport and migration processes with a molecular picture.

Further reading:

1. *N.F. Aguirre, J. Jung, P. Yang. Unraveling the structural stability and the electronic structure of ThO2 clusters. Phys. Chem. Chem. Phys., 22, 18614 (2020).*
2. *K.E. Knope, M. Vasiliu, D.A. Dixon, L. Soderholm, "Thorium(IV)-selenate clusters containing an octanuclear Th(IV) hydroxide/oxide core," Inorg. Chem., 2012, 51, 4239.*
3. *K.E. Knope, R.E. Wilson, M. Vasiliu, D.A. Dixon, L. Soderholm, "Thorium(IV) molecular clusters with a hexanuclear Th core," Inorg. Chem., 2011, 50, 9696.*
4. *D. Hudry, C. Apostolidis, O. Walter, T. Gouder, E. Courtois, C. Kübel, D. Meyer, "Controlled synthesis of thorium and uranium oxide nanocrystals," Chem. Eur. J., 2013, 19, 5297.*
5. *H. Zhang, J.F. Banfield, "Thermodynamic analysis of phase stability of nanocrystalline titania," J. Mater. Chem., 1998, 8, 2073.*
6. *V.M. Samsonov, N.Y. Sdobnyakov, A.N. Bazulev, "On thermodynamic stability conditions for nanosized particles," Surf. Sci., 2003, 532-535, 526.*

Acknowledgments

This work is a collaborative effort with Ping Yang and Julie Jung who played vital roles initiating and contributing to this project respectively. P. Y. was sponsored by the US Department of Energy, Chemical Sciences, Geosciences, and Biosciences Division, Heavy Element Chemistry program, under contract DE-AC52-06NA25396. Financial support was provided by the US Department of Energy through the LANL/LDRD program and the Glenn T. Seaborg Institute for the postdoctoral fellowship to Nestor Aguirre.

David Baumann was a Seaborg Fellow from October 2016–September 2018. His advisors were Pete Silks and John Gordan. He is currently a Research and Development Chemist at Frontier Scientific, Inc.

Creating a New Class of Actinide Chelators

David O. Baumann
Los Alamos National Laboratory, Los Alamos, New Mexico 87545

Plutonium is known to be highly toxic in vivo. Much of this toxicity stems from the high alpha activity of the major isotope ^{239}Pu ($t_{½}$ = 24,000 years), which causes far more damage inside the body compared to outside due to the nature of its alpha decay. Plutonium can displace iron internally and is transported to the liver by transferrin, an iron transport protein. Once plutonium migrates to the liver and lungs it is very slowly eliminated from the body, leading to long-term chronic exposures even with small doses.

Exposure to plutonium and other transuranic elements, such as americium, is typically treated by chelation therapy which can cause severe side effects due to depletion of bio-essential metal cations. Salts of diethylenetriamine-pentaacetic acid (DTPA; Fig. 1c) are FDA-approved to treat exposures to actinides such as plutonium, americium, and curium. DTPA was used to successfully treat an americium exposure in a 1976 accident at the Hanford site that most likely would have been fatal without DTPA chelation therapy.

Currently used chelating agents are often problematic due to side effects and their poor ability to remove actinides deposited in the bones and liver, requiring prompt administration of the drug after exposure and continued doses in the case of large acute exposures in order to minimize deposition in the skeletal system and liver. Highly efficient chelating agents with properties such as tunable selectivity for actinide separations, good bioavailability, low toxicity, and strong binding affinity have long been sought for actinide ions.

Siderophores as effective chelators

Siderophores are high-affinity chelating ligands secreted by microbes to capture Fe^{3+} ions. Many siderophores are known, most notably enterobactin and desferrioxamine B. The former, enterobactin, is the strongest Fe^{3+} chelator currently known, while the latter, desferrioxamine B, is used clinically for the treatment of iron poisoning. The high affinity of siderophores for Fe^{3+} ions stems from its "hard" functionalities such as catecholates and hydroxamates (hard and soft are chemical terms which describe the polarizability of the donor atoms in a ligand; strong bonds result when there is a good match between donor and acceptor hardness). Multiple chelating moieties are arranged with proper orientation for effective binding thus exploiting the chelate effect (Fig. 1; the chelate effect is a phenomenon which enhances the affinity of a ligand when multiple donor groups are present).

Actinide cations such as Pu^{4+}, U^{4+}, and Th^{4+} are hard Lewis acids and preferentially bind to hard Lewis base type ligands such as those found in siderophores. These chelators have been shown to solubilize PuO_2, which is considered to be insoluble under normal conditions and has been implicated in environmental mobilization of Pu(IV). Some siderophores, such as desferrioxamine B, have exceedingly high affinities for Pu^{4+} ions. We can use Fe^{3+} compounds as non-radioactive and non-toxic surrogates for Pu^{4+} species because some of their coordination chemistry and

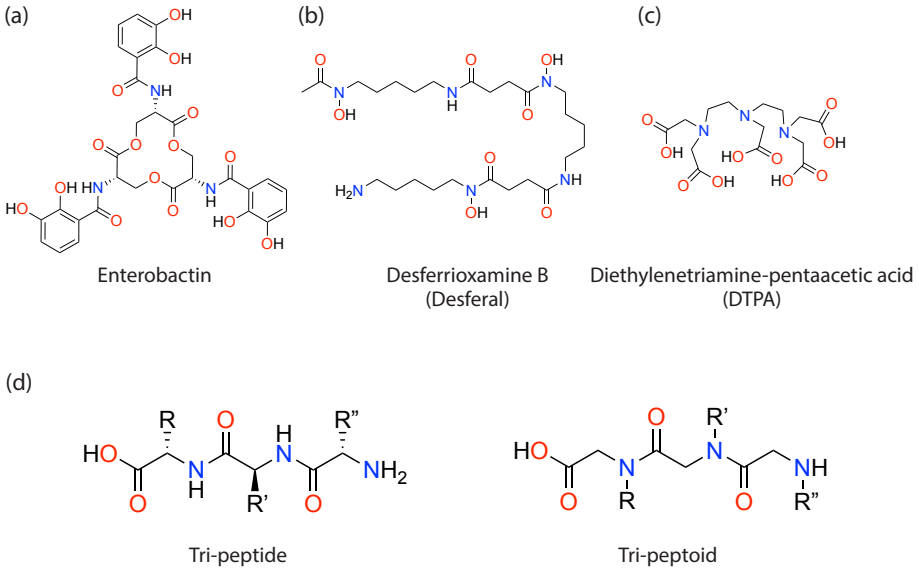

Figure 1. Types of chelators. Structures of: (a) Enterobactin, a triscatechol-based siderophore secreted by Escherichia coli which consists of a 12-membered tri-ester core with pendent catecholate groups; (b) Desferrioxamine B (Desferal) a hydroxamate-based siderophore secreted by *Streptomyces pilosus* used clinically for the treatment of iron overdose; (c) Diethylenetriamine-pentaacetic acid (DTPA), a synthetic actinide chelator used clinically to treat poisoning from actinides such as plutonium and americium; (d) Structural differences between peptides (*left*), which are polymers of natural amino acids from which proteins are made, and peptoids (*right*), which are synthetic polymers composed of N-alkylated glycine monomers (R can be variable).

• • •

biological transport properties are similar—for instance, the charge-to-ionic-radius ratio is 4.3 for Pu^{4+} and 4.6 for Fe^{3+}. Both cations prefer to bind to hard electron donors such as oxygen-containing ligands.

Peptoids are a more robust alternative

While siderophores are potentially good therapeutic candidates for actinide chelation, efficacy of currently FDA-approved siderophores for actinide chelation in vivo is poor. High metal-affinity siderophores, such as enterobactin, suffer from weak linkages in the molecular scaffold that easily undergo hydrolytic degradation in vivo. In a quest for new, highly efficient, and biocompatible chelating agents, peptoids were identified as suitable platforms for the modular assembly of siderophore-like molecules. Peptoids are nitrogen-substituted polymers of the common amino acid glycine. Unlike peptides, which are the sub-units of biologically ubiquitous proteins, peptoids are resistant to degradation under physiological conditions. While unnatural amino acid building blocks for the synthesis of peptides are also resistant to hydrolytic degradation, their synthesis is not trivial due to enantioselective C–C bond formation (enantioselective means to produce a molecule in a preferential geometry or symmetry; it is typically a challenging operation for chemists). Peptoids also lend themselves to extensive chemical diversification due to facile alkylation of a near-infinite number of amine precursors with derivatives of bromoacetic acid (Fig. 1d).

Synthesis of a peptoid siderophore analogue

Design of a first generation peptoid siderophore analogue began by choosing a suitable scaffold that could be readily assembled using traditional synthetic methods

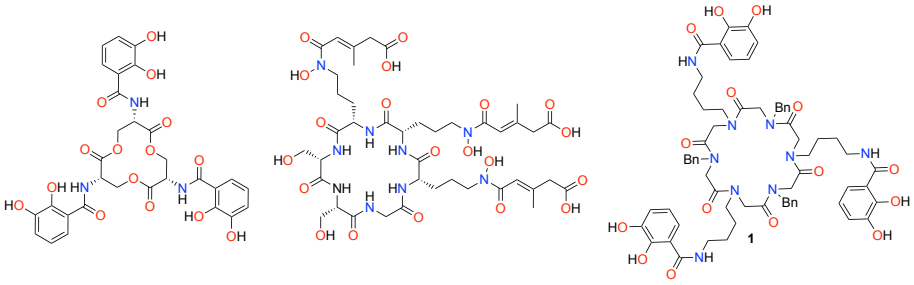

Figure 2. The proposed cyclic peptoid-based siderophore analogue (**1**) is based on the tris-catechol moieties in enterobactin and is a peptoid analogue of the ferrichrome A scaffold.

• • •

and with suitable functionality to attach metal-chelating groups. Cyclic hexameric peptoids have been previously reported in the literature and therefore we chose this system for both a siderophore analogue. A similar peptide-based macrocycle is found in ferrichrome A, which is a hydroxamate-functionalized siderophore. Catecholate functionalities were chosen as metal-binding groups due to their high binding-affinities for Fe^{3+} and actinide ions, their ability to form anionic water-soluble complexes, and their similarity to the metal-binding ligands of enterobactin. Butane-amine side chains were chosen to allow conformational flexibility in the linkers between the peptoid and catecholate groups. Benzyl groups were chosen as synthetic "placeholders" in the final ring structure which could be replaced later with attachment to a resin or antibody, for example. This peptoid hybrid analogue of enterobactin and ferrichrome A is shown in Fig. 2.

To synthesize a complex molecule such as this siderophore analogue, retro-synthetic analysis was performed by conceptually breaking the target molecule into simpler synthons which could be accessed more easily from commercially-available chemicals. Retrosynthesis is the analytical process of working backward from a target molecule to smaller molecules, termed synthons. In this case, the siderophore analogue was reduced to monomeric nitrogen-alkylated glycine fragments via successive disconnections. Following optimization of several different reactions, milligram quantities of the desired siderophore analogue were successfully obtained by a 13 step synthetic route. The ability of the new siderophore analogue to bind Fe^{3+} (in the form of iron(III) triflate) was demonstrated by UV-visible spectroscopy (Fig. 3).

Summary

The liquid phase synthesis of a peptoid-based siderophore analogue was accomplished in 13 steps. This synthesis leads to multiple siderophore analogues, allowing us to relate metal binding affinity to functionality. Therefore, incremental improvements to binding affinity can be made by adjusting the design of future analogues. The tris-catechol derivative was chosen as an initial synthetic target because tris-catechol-based siderophores such as enterobactin are known to have excellent affinity towards Fe^{3+}, a surrogate for Pu^{4+}. UV-visible spectroscopy was used to demonstrate the ability of the siderophore analogue to bind Fe^{3+}. Further studies will elucidate the binding affinity to Fe3+, along with light actinide ions such as U^{4+} and Th^{4+}. An understanding of the binding characteristics of this scaffold to these metals will in turn lead to the rational design of improved analogues.

Acknowledgments

Funding for this work was provided by the US Department of Energy through the Glenn T. Seaborg Institute for Transactinium Science and the Los Alamos National Laboratory LDRD Program (Charlie Strauss principal investigator). Special thanks to Bob Williams and John Gordon for scientific advising and Jurgen Schmidt for help with designing the syntheses and mass spectrometry.

Further reading:

1. *K.N. Raymond, E.A. Dertz, S.S. Kim, "Enterobactin: An archetype for microbial iron transport," Proc. Natl. Acad. Sci., 2003, 100, 3584.*
2. *C.J. Carrano, K.N. Raymond, "Ferric ion sequestering agents. 2. Kinetics and mechanism of iron removal from transferrin by enterobactin and synthetic tricatechols," J. Am. Chem. Soc. 1979, 101, 5401.*
3. *J.R. Brainard, B.A. Strietelmeier, P.H. Smith, P.J. Langston-Unkefer, M.E. Barr, R.R. Ryan, "Actinide binding and solubilization by microbial siderophores," Radiochimica Acta, 1992, 58, 357.*
4. *M.P. Neu, J.H. Matonic, C.E. Ruggiero, B.L. Scott, "Structural characterization of a plutonium(IV) siderophore complex: Single-crystal structure of Pu-desferrioxamine E," Angew. Chem. Int. Ed., 2000, 39, 1442.*
5. *H. Boukhalfa, S.D. Reilly, M.P. Neu, "Complexation of Pu(IV) with the natural siderophore desferrioxamine B and the redox properties of Pu(IV)(siderophore) complexes," Inorg. Chem., 2007, 46, 1018.*
6. *A.E.V. Gorden, J. Xu, K.N. Raymond, "Rational design of sequestering agents for plutonium and other actinides," Chem. Rev., 2003, 103, 4207.*
7. *S.M. Miller, R.J. Simon, S. Ng, R.N. Zuckermann, J.M. Kerr, W.H. Moos, "Comparison of the proteolytic susceptibilities of homologous L-amino acid, D-amino acid, and N-substituted glycine peptide and peptoid oligomers," Drug. Development Research, 1995, 35, 20.*
8. *S.B.Y. Shin, B. Yoo, L.J. Todaro, K. Kirshenbaum, "Cyclic peptoids," J. Am. Chem. Soc., 2007, 129, 3218.*

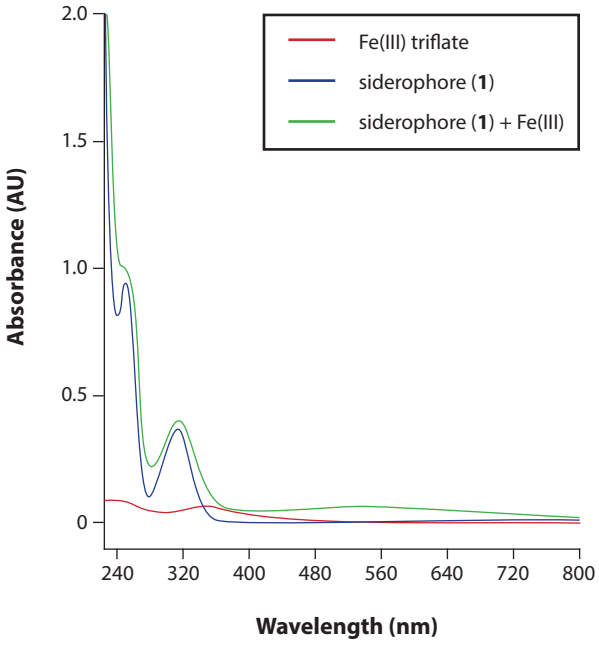

Figure 3. Demonstration of the binding ability of siderophore analogue (**1**) towards Fe(III) triflate by UV-Visible spectroscopy. The new peaks in the isolated product of the siderophore plus Fe(III) reaction (green line) correspond to those of the free siderophore, therefore indicating that it successfully complexed the iron center.

Taylor Jacobs was a Seaborg Fellow from March 2018–August 2019. His area of interest is microstructure-property relationships in plutonium, with mentors Meghan Gibbs and Clarissa Yablinsky. He is now a staff member in the Materials Science and Technology Division, Nuclear Materials Science Group (MST-16).

Developing Internal Friction Capabilities for Plutonium

Taylor R. Jacobs
Los Alamos National Laboratory, Los Alamos, New Mexico 87545

Understanding the nature of radiation damage in plutonium is of great importance as we seek to safely maintain our aging nuclear weapons stockpile without nuclear testing. The arrangement of atoms in a crystal lattice and its defects are directly tied to material properties such as strength. When engineering a material with desirable properties it is vital to understand and control defects in the form of impurity atoms, dislocation structure, grain size/morphology, and secondary phases in an alloy (Fig. 1). In the field of plutonium research there is particular interest in understanding how radioactive decay influences material properties through the introduction of lattice defects. However, certain defects are difficult to analyze because they are often too small to observe, even with advanced techniques such as high resolution transmission electron microscopy. To analyze these small defects we must turn to our fundamental knowledge of how materials behave when probed with physical and electromagnetic sources (e.g., X-rays, electrons, neutrons, mechanical deformation, heat, or electricity). In particular, internal friction is a notable mechanical spectroscopy technique capable of closing the gaps in our understanding of impurity atom mobility in face-centered cubic δ-Pu. This article discusses how it has the potential to further our understanding of plutonium metallurgy and aging.

Internal friction

Internal friction is defined as the dissipation of mechanical energy connected with anelasticity (i.e., time-dependent elastic deformation) and has been used as a method of characterizing metals for over 200 years. In 1912, Charles-Eugène Guye detailed the early history of internal friction testing, starting with Coulomb's elasticity studies using the torsion balance in the late 1700s. Early materials studies using internal friction were performed primarily on iron or steel wires; however, significant controversy arose in the scientific community from the interpretation of results. Breakthroughs in understanding defects in metals using internal friction began in the 1930s when Jacob L. Snoek proposed that interstitial carbon atom diffusion in body-centered cubic α-Fe was directly related to features in the internal friction spectra. Subsequently, internal friction has been used to examine a variety of metallic defects and phase transformations related to nearly every element in the periodic table. Nevertheless, the only internal friction data published for plutonium is a study of the five allotropic phase transformations in which defects were not evaluated.

Physically, internal friction is a measure of mechanical damping during bulk material vibrations—think of a tuning fork (Fig. 2). The exponential decay in vibration is significantly influenced by the testing temperature and frequency as well as the sample crystal structure and mobile defect species present (see Fig. 1 for examples). When internal friction is measured at various temperatures and/or frequencies, peaks are often observed. Peaks occur in the internal friction spectra when the sample temperature is sufficient to overcome the defect specific activation energy. This enables the defect to move within the lattice at the same frequency as the material being vibrated. Therefore peaks will occur at different temperatures and frequencies when defects have different diffusivities, allowing them to be analyzed independently. Peak magnitudes are related to the relative defect concentration.

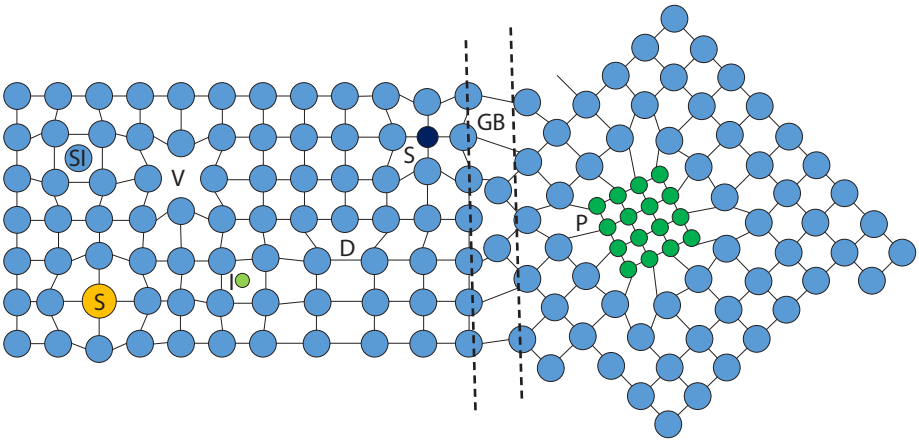

Figure 1. Defects commonly found in metallic crystals, including: interstitial atom (I), self-interstitial atom (SI), substitutional atom (S), vacancy (V), edge dislocation (D), grain boundary (GB), and precipitate or secondary phase (P) defects.

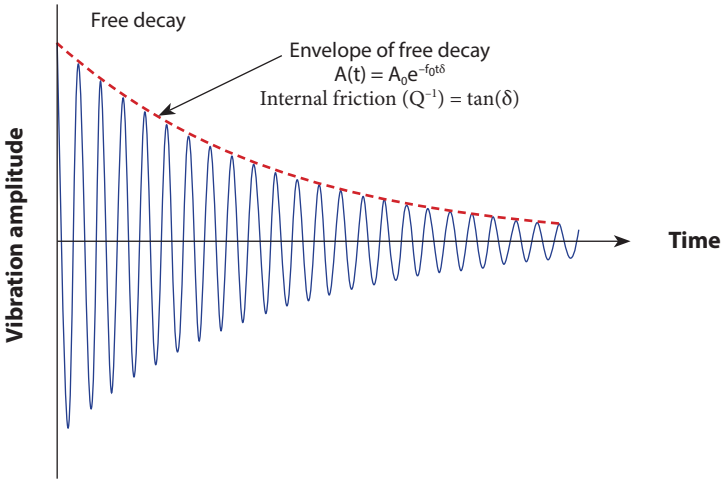

Figure 2. Decay in vibration amplitude (blue line) and envelope of free decay (red dotted line) used to measure internal friction (Q^{-1}). In the envelope of free decay, A is the amplitude, A_0 is the initial amplitude, f_0 is the vibrational frequency, t is time, and δ is a fitting parameter that is directly related to Q^{-1}.

• • •

On the following page are shown examples of internal friction spectra in two HT9 ferritic stainless steels and a schematic diagram of the body-centered cubic lattice defects detected (Fig. 3). Three of these peaks were related to interstitial atoms. The Snoek-Kê-Köster (SKK) peak is related to diffusion of interstitial carbon and/or nitrogen atoms trapped at dislocation cores (see the carbon atom within the edge dislocation in Fig. 3b). The C- and N-Snoek peaks correspond to diffusion of free interstitial carbon and nitrogen atoms respectively. This demonstrates that the internal friction data can highlight the specific defects present and their locations within the crystal lattice. For example, the low nitrogen HT9 steel does not have any detectable free nitrogen (given by the absence of the N-Snoek peak) and most of the carbon interstitial atoms are located in octahedral sites since the C-Snoek peak (related to free interstitial carbon) has a greater magnitude than the SKK peak. The

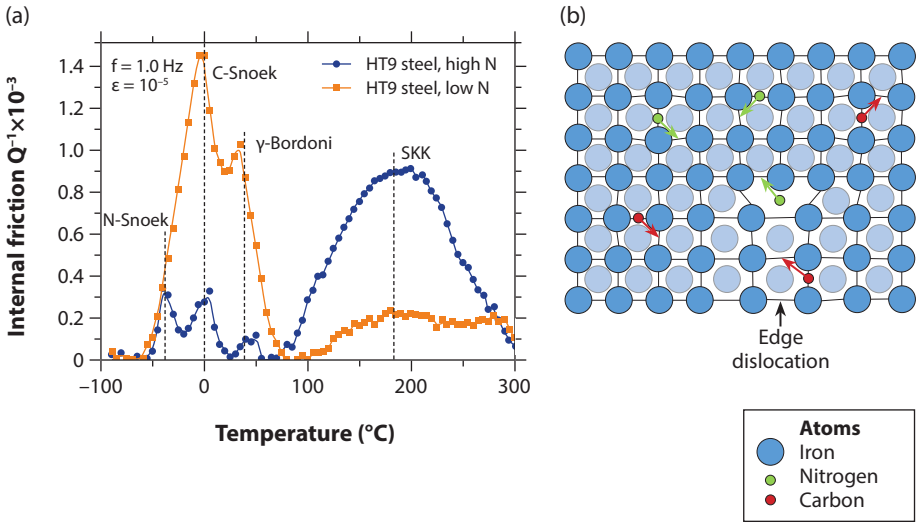

Figure 3. (a) Internal friction (Q^{-1}) spectra of two HT9 stainless steel materials (background subtracted); (b) Base-centered cubic lattice defects detected with internal friction. Arrows represent the diffusion of interstitial atoms within the lattice. N- and C-Snoek peaks in the internal friction spectra are related to diffusion of free nitrogen and carbon interstitial atoms respectively. The γ-Bordoni peak is related to kink formation in dislocations; the Snoek-Kê-Koster (SKK) peak is related to diffusion of carbon or nitrogen interstitial atoms trapped at dislocation cores (see the carbon atom trapped at the edge dislocation).

• • •

high nitrogen HT9 steel has both carbon and nitrogen in the lattice, but most of the interstitial atoms are located at dislocation cores since the SKK peak is much larger in magnitude than the C- and N-Snoek peaks.

Properties of plutonium relevant to internal friction

Pure plutonium has a monoclinic crystal structure (α-Pu) at room temperature and has five allotropic phase transformations before melting at 639°C. It is typically alloyed with gallium to stabilize the higher temperature face-centered cubic phase (δ-Pu; see Fig. 4 on facing page). Since internal friction is sensitive to crystal structure, the temperature ranges of phase stability are important to determine the possible testing conditions. These temperature ranges are relatively small for each phase, making defect analysis of pure plutonium challenging since only a small portion of the spectra can be analyzed. For example, the red arrows in Fig. 4 demonstrate the approximate temperature range where the internal friction spectra could be evaluated in the δ-Pu phase at different gallium concentrations. The δ-Pu phase in pure plutonium is stable over a temperature range of less than 200°C. However, when a few percent of gallium is added, the temperature range available for internal friction analysis is greater than 500°C. The wider temperature range for δ-Pu stability increases the probability of finding defect-related internal friction peaks. Upcoming work will therefore focus on δ-phase Pu-Ga alloys.

Plutonium-239 radioactively decays into uranium-235 and helium-4 (i.e., an alpha particle) with a half-life of 24,100 years. The decay process changes the chemical composition of the alloy and releases 5.2 MeV of energy, some of which is released as kinetic energy when the daughter products collide with atoms in the lattice. Collisions of uranium and helium atoms in the lattice cause a variety of point

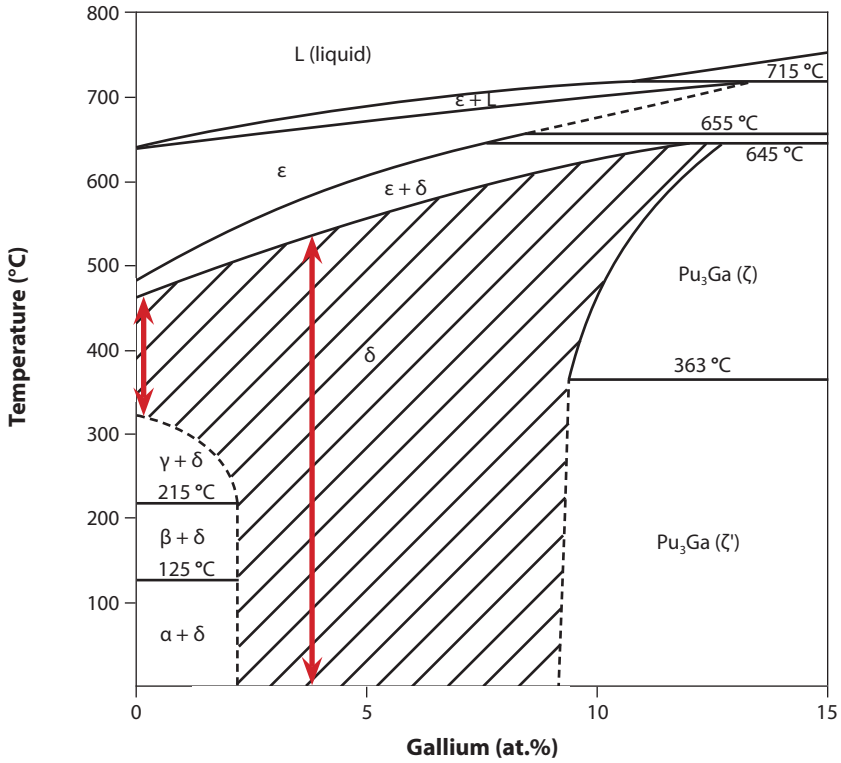

Figure 4. The Pu-Ga phase diagram. Red arrows indicate the temperature range where the δ-Pu phase can be interrogated using internal friction in pure Pu and a delta-stabilized alloy.

• • •

defects, dislocations, and eventually helium bubbles. Additionally, some of the defects generated are mobile and can annihilate each other (i.e., annealing) at material storage temperatures. For example, a self-interstitial plutonium atom can diffuse into a vacancy, annihilating both defects. The constantly evolving defect population can significantly influence the material properties over time, which is why understanding the nature of radiation damage in plutonium is of great importance as we seek to safely maintain our nuclear weapons stockpile without nuclear testing.

Our goal is to characterize plutonium defects that evolve during aging with these internal friction methods. Defect peaks have yet to be studied in plutonium so it is important to first develop a hypothesis describing the peaks that may be present in face-centered cubic δ-Pu. It is also imperative to identify any peaks detected in the first Pu internal friction spectra. Table 1 outlines the potential internal friction peaks that may be observed in δ-Pu based on data from other face-centered cubic metals along with potential methods of identifying each peak. It is anticipated that only some of the peaks summarized will actually be detected experimentally. Early analysis of δ-Pu internal friction spectra can be supported by other ongoing experimental and modeling studies of defects in plutonium. For example, fellow researchers at Los Alamos National Laboratory (LANL) are studying and modeling gallium diffusion in δ-Pu. Activation energies for gallium diffusion found in these studies can be used to calculate theoretical temperature-frequency conditions for a gallium internal friction peak.

Table 1. Internal friction peaks anticipated in δ-Pu according to theory.

Q^{-1} peak	Defect type	Source	Interrogation method
Uranium	Substitutional atoms (low mobility)	Decay product	Test alloys at different ages (concentration increases with age).
Plutonium	Plutonium self-interstitials	Decay product	Test alloys at different ages when stored at low temperatures to prevent Pu diffusion.
Helium	Interstitial atoms (high mobility) or bubbles	Decay product	Bubbles will not likely provide Q^{-1} signal. Low solubility of He in Pu and highly mobile. Peaks are likely at low temperatures and frequencies.
Dislocation kink formation	Screw, edge, or loops	Plastic deformation	Dislocation density increases with strain. Helium bubbles are known to produce loops in face-centered cubic metals. Test a single alloy at different strains and/or ages.
Dislocation or vacancy creep	Dislocation or vacancy motion	Creep	Test multiple samples of a single alloy within the Coble creep (vacancy diffusion) and dislocation creep regimes.

Summary

Internal friction is a powerful characterization technique that uses mechanical deformation to probe crystalline defects and defect structures that are difficult to account for with more traditional methods. We have installed a dynamic mechanical analyzer (DMA) capable of measuring internal friction in non-radioactive metals as a proof of concept to lead into plutonium testing. Specifically, internal friction has the potential to quantitatively detect movement of gallium, uranium, helium, vacancies, plutonium self-interstitials, and dislocation kinks. Successfully characterizing the evolution of these defects during aging will be a significant accomplishment in the field of plutonium metallurgy, as many of these phenomena have remained elusive experimentally. Designs to incorporate a DMA into a glovebox for plutonium testing are ongoing—installation in LANL's Plutonium Facility (PF-4) will result in the first internal friction instrument capable of testing plutonium in over 50 years.

Acknowledgments

This work was a collaborative effort which benefited from significant contributions from the following scientists: Clarissa A. Yablinsky (MST-16), Tarik A. Saleh (MST-8), Meghan J. Gibbs (MST-16), Franz J. Freibert (NSEC), and Boris A. Maiorov (MPA-MAG). Funding for this work was provided by the US Department of Energy through the Glenn T. Seaborg Institute and LDRD at Los Alamos National Laboratory for the postdoctoral fellowship for Taylor R. Jacobs.

Developing Accident Tolerant Nuclear Fuels

Temperature-Dependent Properties of UO_2 and U_3Si_2

Jordan A. Evans
Los Alamos National Laboratory, Los Alamos, New Mexico 87545

In 2011 the Japanese Fukushima-Daiichi nuclear power station experienced a catastrophic core meltdown following the 9.0 MW offshore Tōhoku earthquake and tsunami. It was the most severe nuclear accident since the Chernobyl disaster in 1986, and the only other accident to receive the Level 7 event classification of the International Nuclear Event Scale. Following this, the US Department of Energy (DOE) has directed additional resources toward the development of accident-tolerant nuclear fuel (ATF) concepts for current light water-cooled nuclear reactors (LWRs). Many ATF candidates are under consideration: see the 2016 Nuclear Engineering and Design article entitled "Sensitivity study for accident tolerant fuels: Property comparisons and behavior simulations in a simplified PWR to enable ATF development and design" for several detailed comparisons.

Uranium dioxide (UO_2) is arguably the most thoroughly studied actinide compound due to its exclusive use as commercial nuclear reactor fuel. UO_2 has properties that make it a useful nuclear fuel in commercial LWRs, such as high melting point (~3140 K), thermal stability, chemical stability in the presence of both fission products and high temperature H_2O coolant, excellent neutronic properties, and low radiation-induced swelling. UO_2 is also relatively easy to fabricate in comparison to most other candidate nuclear fuels.

Thermal conductivity is one of the most important factors in nuclear fuel performance—i.e., the ability of the fuel to transfer thermal energy produced from fission. UO_2 has poor thermal conductivity (2–3 $W{\cdot}m^{-1}{\cdot}K^{-1}$ in reactor operating conditions) compared with other nuclear fuel candidates. As the temperature of the fuel increases, the thermal conductivity of UO_2 decreases, effectively resulting in a feedback mechanism which can further lead toward meltdown. This undesirable behavior occurs, in spite of its increasing heat capacity with temperature, due to the increasingly poor diffusivity of thermal energy as the temperature increases.

In this work, the ATF candidate U_3Si_2 was also investigated. Although U_3Si_2 has a lower melting point (~1935 K), its thermal conductivity at normal reactor operating conditions is 25–30 $W{\cdot}m^{-1}{\cdot}K^{-1}$, nearly an order of magnitude higher than that of UO_2. The thermal conductivity of U_3Si_2 further increases with temperature. U_3Si_2 is therefore believed to be more resistant to meltdown than UO_2 despite its lower melting point. Additionally, U_3Si_2 has a uranium density of 11.31 $gU{\cdot}cm^{-3}$, while UO_2 has a lower uranium density of 9.66 $gU{\cdot}cm^{-3}$. Even after considering differences in neutronics, the use of U_3Si_2 fuel would allow for less frequent refueling outages than the same reactor using UO_2 fuel without increasing the fuel enrichment. This means that reactors using U_3Si_2 fuel would be more economically competitive than those using UO_2 fuel.

Jordan Evans was a Seaborg Fellow from June 2018–May 2020 working under the mentorship of Boris Maiorov and Marcelo Jaime. He is currently a Staff Scientist in the Nuclear Materials Department at Idaho National Laboratory. His research interests include the design and irradiation performance of textured nuclear materials, nuclear fuel, cladding, and structural materials for use in extreme conditions, and the implementation of nanotechnology in nuclear systems and nuclear medicine.

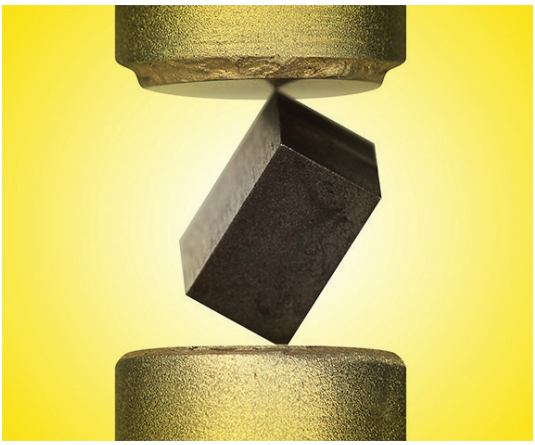

Figure 1. A sample held between the two transducers during a resonant ultrasound spectroscopy (RUS) experiment. One transducer mechanically excites the sample over a range of ultrasonic frequencies, while the other transducer records the sample's response.

• • •

U_3Si_2 has not been scrutinized to the same level as UO_2 as a reactor fuel, and many of its temperature-dependent thermomechanical properties have never been measured, including the elastic constants and the Grüneisen parameter (introduced later in the article). Additionally, the elastic constants of conventional UO_2 have not been measured since the 1960s, and updating these values will improve DOE simulation codes used to predict nuclear reactor performance and safety.

Heat transfer and elasticity

Ceramic nuclear fuels such as UO_2 are wide-gap insulators. As such, heat transfer is dominated by elastic wave lattice vibrations. In the field of quantum mechanics, these lattice vibrations are composed of quasiparticles known as "phonons". Phonons can scatter with other particles, including electrons, magnons (quasiparticle spin-waves), and other phonons, increasing the amount of time it takes phonons to carry their energy from one part of the material to another. The thermal conductivity of a material can be determined at any temperature as the sum of the contributions of all of the active phonon modes, which are strongly dependent upon the elastic properties of the material, i.e., Hooke's law (see the 2004 Technical Physics Letters article "The acoustical Grüneisen constants of solids" for more details). In other words, the thermal conductivity of a ceramic is strongly dependent upon its elastic properties. The most general form of Hooke's law, which does not assume that elastic properties are the same in every direction, is written in the language of tensor mathematics to linearly relate the stresses and strains in a material by a set of 21 independent elastic constants, c_{ij}. Fortunately, as-fabricated ceramic nuclear fuel is highly isotropic when it is produced via conventional pressing and sintering of powders (isotropic means that the property has the same value when measured in different directions), which results in a pellet density that is ~95% that of the theoretical maximum. This simplifies the elastic tensor as there are only two independent elastic constants, c_{11} and c_{44}, the compressive and shear elastic constants, respectively. These elastic constants can also be used to directly determine a variety of other important thermomechanical quantities, including engineering constants (Young's modulus, bulk modulus, shear modulus, and Poisson's ratio) and the Grüneisen parameter.

Resonant ultrasound spectroscopy

One method of measuring the elastic constants of a solid takes advantage of the principles of vibrational harmonics. If the geometry and density of a material are known, and its resonance frequencies are measured, then the entire elastic tensor c_{ij} of the material can be determined. The experimental technique by which the resonance frequencies are measured is known as resonant ultrasound spectroscopy (RUS). Qualitatively, the RUS experiment is quite simple. The sample is placed between two transducers (Fig. 1). One transducer is essentially a speaker which mechanically excites the sample at an ultrasonic frequency, while the other transducer acts as a microphone to measure the sample's response. The excitation frequency is swept, typically from tens of kHz to several MHz, in order to obtain a spectrum containing a large set of resonance frequencies. The entire spectrum can be measure typically within a minute or two, and can be repeated continuously while changing the sample's environment (i.e., temperature, externally applied magnetic field strength, etc.). A resonance frequency is found when the recorded response of the material "spikes" at a particular frequency (see Fig. 2 for an example of a resonant ultrasound spectrum of UO_2).

The resonance frequencies measured in RUS can be used to determine the entire elastic tensor of the material even if its properties are not isotropic, meaning that RUS is a symmetry-sensitive technique which detects anisotropy (which could come from texture, oriented fiber reinforcement, single crystal samples, etc.). RUS is a very sensitive technique (one part in 10^6 or better), detecting changes in physical properties including density, thermal expansion, elastic properties, sound speeds, and geometry. When the local temperature of the environment changes up or down, a solid sample expands or contracts by the thermal expansion coefficient (delta length/initial length ~ one part in 10^6 or more). This is easily observed by RUS. It also does not require the use of adhesives or mounts, simplifying experiments to be performed on hazardous or radioactive materials.

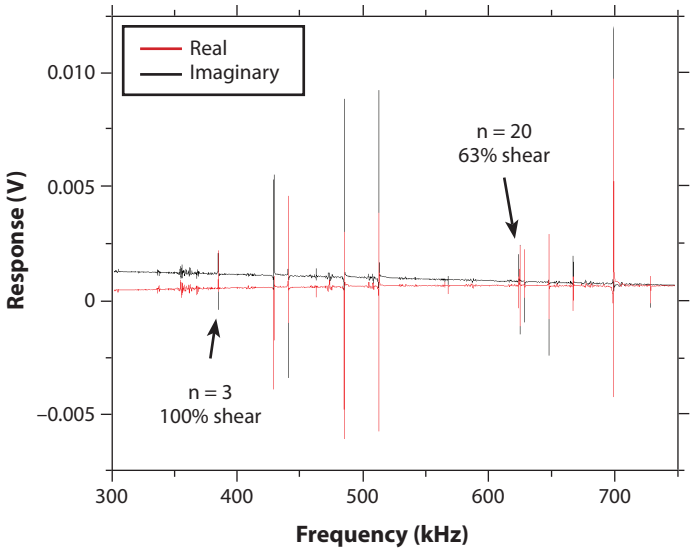

Figure 2. Resonant ultrasound spectrum of an as-fabricated polycrystalline UO_2 sample at 240 K, where the n = 3rd resonance is pure shear force and n = 20th resonance is 63% shear. These frequencies can be used to calculate the elastic tensor c_{ij}.

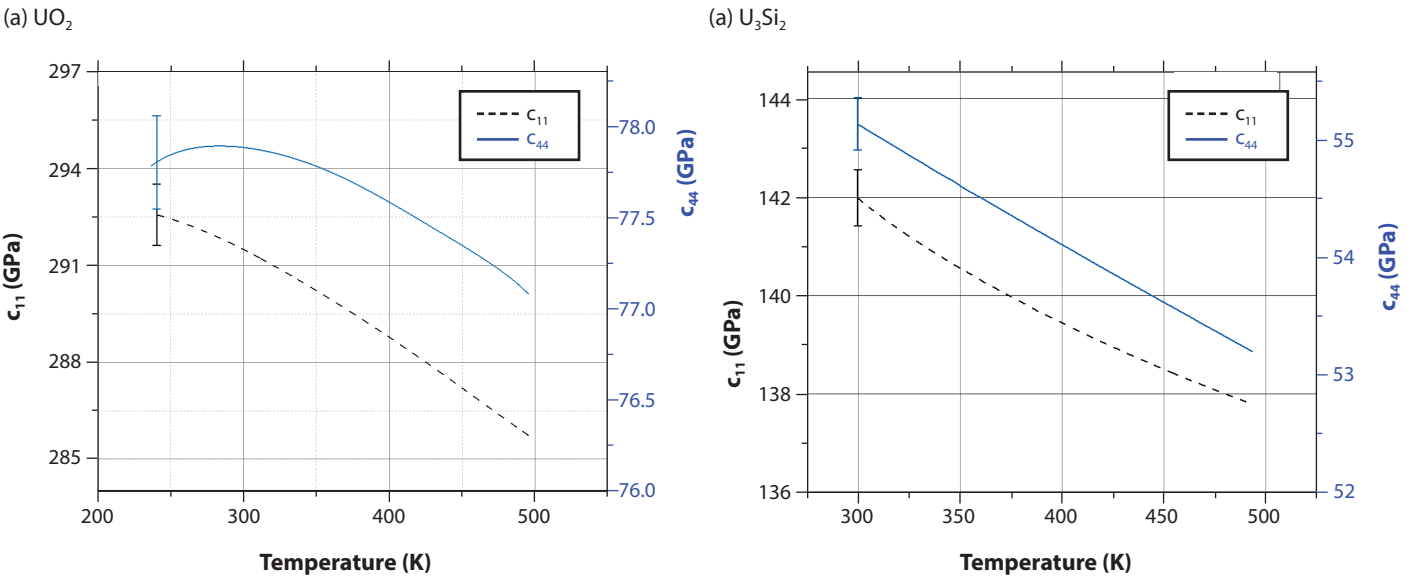

Figure 3. The elastic constants c_{11} and c_{44} versus temperature for: (a) as-fabricated polycrystalline UO_2. The decrease in values of c_{44} below room temperature is due to strong magnetoelastic coupling as the material approaches the paramagnetic-antiferromagnetic transition at 30.8 K. The error bars may appear unusual at first glance, but represent the difference between "accuracy" and "precision". (b) For as-fabricated polycrystalline U_3Si_2.

Independent elastic constants of UO_2 and U_3Si_2

Typically, the elastic constants of materials vary with temperature according to the Varshni model (assuming there are no phase changes), whereby c_{11} and c_{44} are constant at cryogenic temperatures, then decrease linearly with increasing temperature. Temperature-dependent behavior which does not follow the behavior predicted by Varhsni indicates that there are underlying mechanisms that are coupled to the thermoelastic properties of the material.

UO_2 has been studied extensively in the past and is known to disobey the Varshni model (Fig. 3a). In an RUS experiment, the elastic properties of a material are determined at a given temperature (240 K in this case), which is associated with a given error indicated by the error bar (0.4%). The decrease in c_{44} as temperature decreases below room temperature disobeys the Varshni model, as to be expected. This is due to strong magnetoelastic coupling in UO_2 as the temperature approaches the paramagnetic-antiferromagnetic transition at 30.8 K.

We measured the temperature-dependent elastic constants (c_{11} and c_{44}) of U_3Si_2 for the first time (Fig. 3b). At a glance, they appear to be well-behaved according to the Varshni model. Elastic properties of U_3Si_2 were not explored below room temperature, hence we did not observe the elastic constants approaching constant values at cryogenic temperatures. Looking more closely at the compressive elastic constant, c_{11}, however, we notice slight upward curvature. This is more obvious when looking at the derivative of c_{11} with respect to temperature which reveals anomalous upward curvature. While this change is subtle, it is contrary to the behavior predicted by the Varshni model and may be indicative of an as-yet unknown phenomenon that is coupled with the elastic behavior of the material.

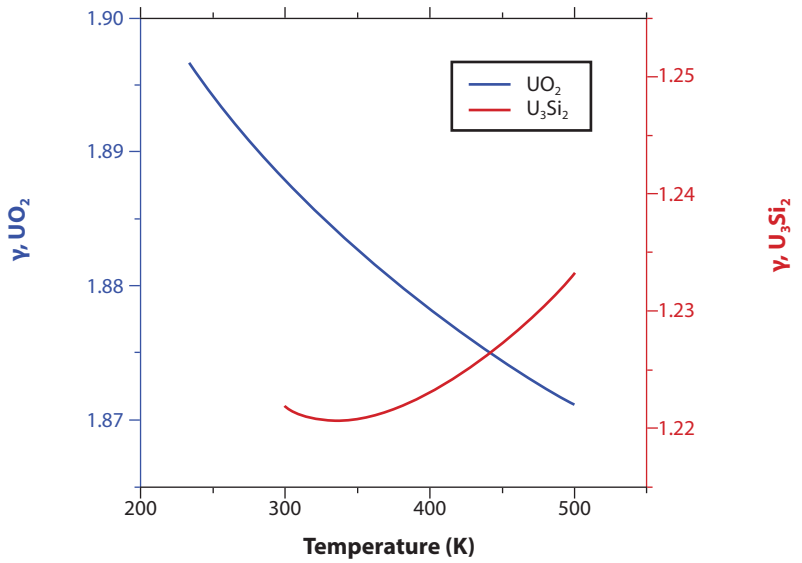

Figure 4. The temperature-dependent Grüneisen parameters for as-fabricated polycrystalline UO_2 (blue) and U_3Si_2 (red), as calculated directly from the measured elastic constants c_{11} and c_{44}. We see completely different behavior for these two materials, which challenges the conventional wisdom.

The Grüneisen parameter

The Grüneisen parameter, γ, is a dimensionless quantity used in materials science. It is a combination of other familiar material properties and describes how changes in temperature influence the dynamical properties of the crystal lattice, including phonon nonlinearities. There are many formulations of γ, including thermodynamic/macroscopic formulations (which are equivalent due to Maxwell's relations), as well as those which are derived from interatomic/microscopic properties of the lattice. One equivalent formulation of the Grüneisen parameter arises from the elastic properties of the material, and can be calculated directly from the elastic constants of the material. For both UO_2 and U_3Si_2, γ is typically considered to be constant with respect to temperature, with values ranging 1.25–2.0 assumed in the literature.

We successfully determined temperature-dependent Grüneisen values using our measured elastic constants for UO_2 and U_3Si_2 (Fig. 4, above). Two immediate observations became apparent: (1) γ is not constant with respect to temperature for both materials, and (2) the temperature-dependent behavior of γ for UO_2 and U_3Si_2 are completely different. For UO_2 above room temperature, γ decreases, while for U_3Si_2, it increases. By linearly extrapolating these values up to reactor operating fuel temperatures (above 1,000 °C), we note that γ changes from room temperature values by more than 5%.

Summary

For the first time in over half a century, the temperature-dependent elastic constants of UO_2 have been measured and show improved accuracy over those obtained in the 1960s. A decrease in the values of the UO_2 elastic constants was observed below room temperature, which is associated with magnetoelastic coupling as the temperature approaches the paramagnetic-antiferromagnetic transition. The temperature-dependent elastic constants of U_3Si_2 have been measured for the first time, revealing anomalous positive curvature of the compressive elastic constant c_{11}. The elastic constants can be used to directly compute various other thermoelastic properties. The data obtained from these experiments not only demands further investigation of the temperature-dependent elastic behavior of U_3Si_2, but also has direct application toward DOE simulation codes which are used to predict the performance and safety of nuclear reactors using these fuels.

Further reading:

1. *Y.P. Varshni, "Temperature dependence of the elastic constants," Phys. Rev. B, 1970, 2(10), 3952.*
2. *O.G. Brandt, C.T. Walker, "Temperature dependence of elastic constants and thermal expansion for UO_2," Phys. Rev. Lett., 1967, 18, 11.*
3. *V.N. Belomestnykh, "The acoustical Grüneisen constants of solids," Tech. Phys. Lett., 2004, 30, 91.*

Acknowledgments

This work was a collaborative interdisciplinary effort which benefited from contributions from the following scientists: Krzysztof Gofryk (Idaho National Laboratory), Ursula Carvajal-Nuñez (MST-8), Joshua T. White (MST-8), Tarik A. Saleh (MST-8), David M. Frazer (MST-8), Jonathan B. Betts (MPA-MAG), Fedor Balakirev (MPA-MAG), Marcelo Jaime (MPA-MAG), and Boris Maiorov (MPA-MAG). Ranging from sample preparation, equipment design, equipment construction/repair, and software design, the contributions from these scientists were critical toward the success of this ongoing work. Financial support was provided by the US Department of Energy through the LANL/LDRD program, and the Glenn T. Seaborg Institute for the postdoctoral fellowship of Jordan Evans.

Employee Spotlight

Sheldon Apgar: A glovebox worker's best friend

Maureen Lunn

Sheldon Apgar is known around TA-55 for being the go-to problem solver for equipment in the Plutonium Facility (PF-4) and other area laboratories. As a designer/drafter in the Actinide Materials Processing & Power (AMPP-4) group, Apgar plays a key role in keeping PF-4 up and running.

In 1996 he joined the Laboratory as a glovebox worker, but because he took a few classes on the drafting and design software AutoCAD in high school it was not long before he was pulled in to help with design projects to improve gloveboxes. He says that when he took the AutoCAD classes, he never thought he would do anything with it. But 24 years later, he is the local AutoCAD expert and has built a career on drafting and design.

On an average day at TA-55, Agpar and his team spend their time designing new equipment used inside gloveboxes—the large, sealed containers that protect workers from special nuclear materials. "Typically, the majority of the equipment we work on is inside the glovebox and known as 'process equipment,'" he says. "The type of equipment we design has to do a certain function that is likely only done at TA-55. This type of work isn't done anywhere else in the world, so we can't go to a catalog to order our equipment."

Watching and learning

Occasionally, the AMPP-4 team designs modifications to make existing equipment work for its purposes. In addition to the physical design, Agpar and his colleagues also have to constantly factor in the atmosphere within the glovebox, including considerations for heat, material characteristics and the possibility for corrosion. Agpar says he is grateful for all the colleagues who have helped him understand the science over the years. "The people I've worked with have always been good to help explain these chemical processes to me, since that has never been my background," he says. "They took the time to show me how things work — not just tell me — and that's helped me to gain a good understanding." Agpar takes the same approach now of showing versus telling. With everyone from his design teammates to technicians working in the facility to students he mentors, he takes the time to slow down and teach others. "It's gratifying to see the next generation come in [to work at the Lab]," he says. "I've been really impressed with their willingness to learn and ask questions."

Focused on supporting the worker

While the job title Designer/Drafter might conjure a picture of someone sitting in front of a computer screen all day, Agpar is known for being on the facility floor, working to understand gloveboxes and the challenges faced by those who work with them. If someone has an issue, he is often the first person to drop what he is doing, head to the glovebox and try to figure out a solution. Getting work done inside a glovebox is no easy feat, and Apgar's approach to design helps workers because he understands the problems from first-hand experience. He describes working in a glovebox as being a constant challenge of restricted dexterity, limited reach, and limited view. Anything from fastening a bolt to tearing a piece of tape is difficult inside a glovebox.

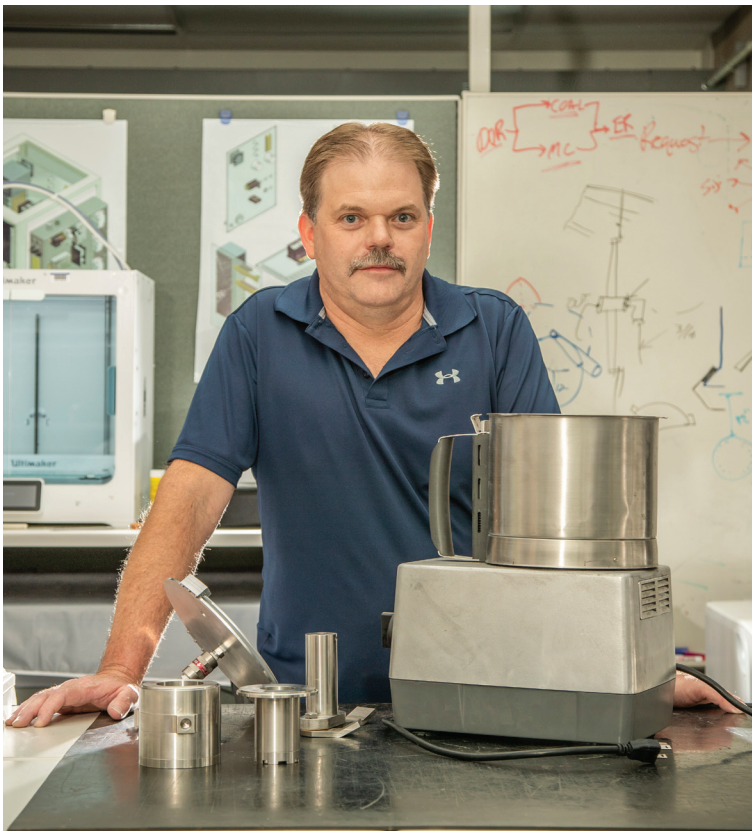

Above, left: Sheldon Apgar in his office at TA-55, where he works as a designer/drafter and has a knack for solving glovebox problems. **Top, right:** Kenny Hansel (*right*) and Ross Thornburg (*left*) (AMPP-3) work in a glovebox with parts that Sheldon helped design. Employees like these work in gloveboxes regularly, which can be a constant ergonomic and technical challenge. **Bottom, right**: Detail of glovebox part.

"Imagine putting your big, heavy winter gloves on, picking up a sewing needle off a table and threading it at arm's length in front of you," he explains. "That would be easier than some of the things that glovebox workers have to do in a glovebox."

Agpar and his team have a reputation around the Laboratory for their innovative solutions to unique problems. From partnering with the Facilities and Operations Directorate for the equipment that benefits glovebox processes, to designing for projects outside of his normal scope of work (such as equipment for waste drum characterization), he has a broad perspective on the work at the Lab and the solutions to improve all sorts of processes.

TA-55 family legacy

Sheldon's father, Stewart Apgar, started working at the Laboratory in 1949. While their jobs never overlapped formally, his dad retired from a group at TA-55 where he also did glovebox work, after working at the old plutonium plant on DP road. Growing up with a parent who worked at TA-55 gave him an early understanding of the atmosphere of working at the Lab. Today, he tries to pass that same sense of a broad understanding on to his colleagues, including student mentees and new employees.

"People come to me with questions because they know I can answer them faster than they can dig it up in a document," Agpar says. "It's important to pass that type of knowledge on."

THE GLENN T. SEABORG INSTITUTE

Actinide Research Quarterly is published by Los Alamos National Laboratory and is a publication of the Glenn T. Seaborg Institute for Transactinium Science, a part of the National Security Education Center. ARQ (est. 1994) highlights research in actinide science in such areas as process chemistry, metallurgy, surface and separation sciences, atomic and molecular sciences, actinide ceramics and nuclear fuels, characterization, spectroscopy, analysis, and manufacturing technologies.

LA-UR-20-30461

Address correspondence to:
Actinide Research Quarterly
c/o Editor
Mail Stop T001
Los Alamos National Laboratory
Los Alamos, NM 87545

ARQ can be read online at:
www.lanl.gov/arq

If you have questions, comments, suggestions, or contributions, please contact the ARQ staff at:
arq@lanl.gov

Los Alamos National Laboratory is operated by Triad National Security, LLC, for the National Nuclear Security Administration of U.S. Department of Energy (Contract No. 89233218CNA000001).

Actinide Research Quarterly
Mail Stop T001
Los Alamos National Laboratory
Los Alamos, NM 87545

arq@lanl.gov

Presorted Standard
U.S. Postage Paid
Albuquerque, NM
Permit No. 532

THE GLENN T.
SEABORG
INSTITUTE